Design of all-optical temporal differentiator using a Moiré fiber grating

Qiong Liu (刘 琼), Qing Ye (叶 青)*, Zhengqing Pan (潘政清), Haiwen Cai (蔡海文), Ronghui Qu (瞿荣辉), and Zujie Fang (方祖捷)**

Shanghai Key Laboratory of All Solid-State Laser and Applied Techniques, Shanghai Institute of Optics and Fine Mechanics, Chinese Academy of Sciences, Shanghai 201800, China

**Corresponding author: yeqing@siom.ac.cn;* ***corresponding author: rhqu@siom.ac.cn*

Received March 19, 2012; accepted April 13, 2012; posted online July 5, 2012

We design and demonstrate an all-optical temporal differentiator based on a simple Moiré fiber grating operated in reflection. The simulation results prove that a single Moiré fiber grating with only one π-phase shifted point can act as the first-order temporal differentiator and that a Moiré fiber grating incorporating two symmetrical π-phase shifted points can act as the second-order temporal differentiator. A practical Moiré fiber grating is fabricated, thereby proving that such a grating can act as the first-order temporal differentiator. Our results verify the feasibility, flexibility, and accuracy of the proposed method.

OCIS codes: 230.1150, 060.3735, 320.7085.
doi: 10.3788/COL201210.092301.

Recently, all-optical circuits implemented for all-optical computing and signal processing have attracted significant attention due to the exponential development of photonics technologies. Such devices operated in the optical domain can provide a wider bandwidth and higher operating speed than devices operated in the conventional-electronics-based system. One of the fundamental devices, the temporal differentiator, has been designed and researched by several groups. A temporal differentiator can transform the field complex profile of an optical signal to its differential signal immediately. Aside from applications in the all-optical computing and signal processing fields, a temporal differentiator has a wide variety of applications in other areas, such as pulse characterization[1,2], femtosecond pulse shaping[3,4], ultrashort pulse train generation[5], and high-speed optical communication[6].

Currently, several technologies have been proposed to realize a temporal differentiator theoretically and experimentally. In general, these reported temporal differentiators can be classified into two categories: incoherent and coherent[7]. Incoherent optical differentiators based on cross-gain modulation in a semiconductor optical amplifier have been reported since 2007[8,9]. The incoherent optical differentiator operates on the optical intensity, instead of the field complex profile, of an initial optical signal. Many methods have been proposed to realize the coherent optical differentiator, including the use of silicon micro ring resonator[10], long-period fiber grating (LPFG)[11,12], and optical interferometer[13]. The silicon micro ring resonator can offer an operational bandwidth in the tens of gigahertzs[10], whereas the experimentally proven differentiator based on LPFG offers operational bandwidth up to many terahertzs. However, the long-period fiber grating is extremely sensitive to environmental changes[7,14]. In addition integral differentiator (the differentiation order is an integer) and fractional differentiators have been proposed since 2008, including the use of a Mach-Zehnder interferometer[15], LPFG[16], and tilted fiber grating[17]. The differentiation order can be continuously adjusted when the tilted fiber grating acts as a fractional differentiator[17]. High-order temporal differentiator can be obtained by concatenating a linearly chirped fiber Bragg grating with the first-order temporal differentiator[18] or by using a long-period fiber Bragg grating that provides full energy recoupling from the cladding mode back into the core mode[11].

In this letter, we design and demonstrate a single Moiré fiber grating to realize an all-fiber temporal differentiator that utilizes the mathematical existence of exact π-phase shifted points when the refractive modulation profile of the Moiré fiber grating passes through the zero point. The operational bandwidth of the proposed method is from many gigahertzs to many tens of gigahertzs. In addition, the Moiré fiber grating has a higher tolerance to the environmental changes than the LPFG. Therefore, our proposed differentiator can be widely used in all-optical communications. The first- and second-order temporal differentiators are designed as examples in this letter. The simulation results prove that a single Moiré fiber grating with only one π-phase shifted point can act as the first-order temporal differentiator. The second-order temporal differentiator is achieved by a Moiré fiber grating incorporating two symmetrical π-phase shifted points. Good waveform matches between the ideal differential signal and the output temporal waveform are recorded for both of the first- and second-order temporal differentiators. Thus, practical Moiré fiber grating is fabricated, thereby proving that such a grating can act as the first-order temporal differentiator.

We suppose that the temporal waveform of the initial input signal is described as $u(t)$, and that the frequency waveform is described as $U(\omega)$. In addition, the temporal waveform of derivative signal can be written as $v(t) = \mathrm{d}^N u(t)/\mathrm{d}t^N$, and $V(\omega)$ is the frequency domain expression of $v(t)$. The basic relationship in the fre-

quency domain between initial signal $u(t)$ and differential signal $v(t)$ is based on the derivative properties of Fourier transform. We can easily prove that the spectral response function of an Nth-order temporal differentiator is given by

$$H(\omega) = V(\omega)/U(\omega) \propto [\mathrm{i}(\omega - \omega_0)]^N, \tag{1}$$

where ω_0 represents the center frequency of initial signal $u(t)$ and $\mathrm{i} = \sqrt{-1}$ is the imaginary unit. Notably, energy depletion occurs at the signal center frequency ω_0. Thus, an exact π-phase jump should be introduced in the center frequency for odd-order temporal differentiator as a result of the existence of imaginary unit. For the first-order differentiator, the amplitude response depends linearly on the frequency; thus, the π-phase jump should be introduced. For the second-order differentiator, the amplitude response function is a parabolic curve.

Using two uniform phase masks with slightly different period superimposed in a conventional photosensitive fiber, a Moiré fiber grating can be fabricated easily. The refractive index modulation of the grating is written as

$$\Delta n(z) = \delta n_1 \Big[1+\cos(\frac{2\pi}{\Lambda_1} z+\phi_1)\Big] + \delta n_2 \Big[1+\cos(\frac{2\pi}{\Lambda_2} z+\phi_2)\Big], \tag{2}$$

where Λ_1 and Λ_2 are the periods of the phase mask, δn_1 and δn_2 are the average refractive index modulations, and ϕ_1 and ϕ_2 are the initial phases of the refractive index modulation corresponding to the first and second fiber gratings, respectively. Conventionally, $\delta n_1 = \delta n_1 = \delta n$; therefore, Eq. (2) can be rewritten as

$$\delta n(z) = 2\delta n + 2\delta n \cos\Big(\frac{2\pi z}{\Lambda_\mathrm{c}} + \frac{\phi_1+\phi_2}{2}\Big) \cdot \cos\Big(\frac{2\pi z}{\Lambda_\mathrm{s}} + \frac{\phi_1-\phi_2}{2}\Big), \tag{3}$$

where $\Lambda_\mathrm{c} = \frac{2\Lambda_1\Lambda_2}{\Lambda_1+\Lambda_2}$ and $\Lambda_\mathrm{s} = \frac{2\Lambda_1\Lambda_2}{\Lambda_1-\Lambda_2}$. Here, a Moiré fiber grating can act as a rapid variable structure (the period is Λ_c) with a slowly varying profile (the period is Λ_s). We can easily prove that the refractive index modulation of the Moiré fiber grating has exact π-phase shifted points when the slowly varying envelope passes through the zero point[19]. The response characteristic of the Moiré fiber grating is decided by the number and the location of the π-phase shifted points. Conventionally, the number of the π-phase shifted points is decided by the period of the slowly varying profile and the length of Moiré fiber grating. The locations of π-phase shifted points depend on the initial phase of the refractive modulation. When the π-phase shifted point is located at the center of the Moiré fiber grating, the resonance dip has a lower reflection, which may cause energy depletion. Therefore, the key point in the design is choosing the rational period and the initial phase of the Moiré fiber grating.

The calculations and analyses following describe the use of a Moiré fiber grating to realize the temporal differentiator. The first- and second-order optical temporal differentiators were designed as examples in this letter. For the Moiré fiber grating, the π-phase shifted point of the refractive index modulation is an equivalent element with a short section of fiber with the π transmission phase. Therefore, the Moiré fiber grating could be treated as an interferometer. As expectation, a narrow resonance dip was found at the center of stopband of the Moiré fiber grating because the phase shift of the refractive index modulation was exactly equal to π. According to the above discussion, the reflection phase of the Moiré fiber grating for the first-order temporal differentiator needs an exact π-phase jump in the center frequency. Therefore, the Moiré fiber grating for the first-order differentiator maintains only one π-phase shift point along the fiber axis. In order to ensure an adequate resonance dip in the center frequency, the initial phase differentia $\phi_1 - \phi_2$ must equal 0, which means that the π-phase shifted point of the refractive index modulation must be located at the center point of the fiber. For the second-order temporal differentiator, the reflection phase does not need a π-phase jump; rather, the Moiré fiber grating incorporates two symmetrical π-phase shifted points.

Figure 1(a) shows the refractive index modulation of the designed Moiré fiber grating for the first-order differentiator. The length of fiber grating was 10 mm and the periods of the fiber grating were 535.481 and 535.51 nm. Therefore, the period of slowly varying profile was approximately 19.8 mm, which means that only one π-phase shifted point existed along the fiber axis. The maximum refractive index modulation was approximately 1×10^{-4}. Because Moiré fiber grating used was a non-uniform fiber grating, calculating the frequency response function with an analytic expression would be difficult. Therefore, a transfer matrix method was applied to calculate the reflection amplitude and phase. Figure 1(b) shows the reflection amplitude and phase of the Moiré fiber grating designed for the first-order differentiator. As expected, a π-phase jump occurred in the center frequency, and the reflection amplitude was approximately linearly dependent on the frequency in the reflection dip. These phenomena demonstrate that the required amplitude and phase features are satisfied for the first-order differentiator. The operational bandwidth of the designed temporal differentiator was limited by the refractive index modulation amplitude. The reflection bandwidth of the Moiré fiber grating became wider with the increasing of amplitude of the refractive index modulation. This phenomenon illustrated that the bandwidth of the resonance dip (the operational bandwidth)

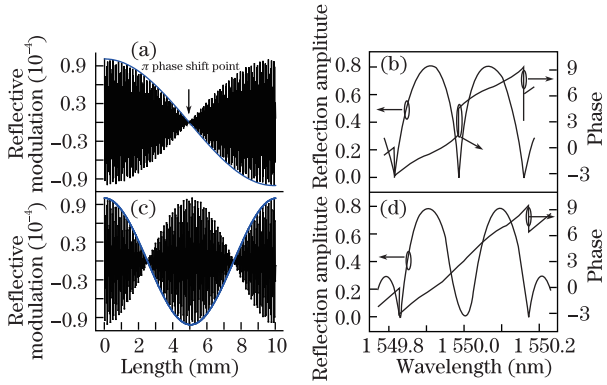

Fig. 1. (a) Refractive index modulation and (b) reflection amplitude and phase of the first-order differentiator; (c) refractive index modulation and (d) reflection amplitude and phase of the second-order differentiator.

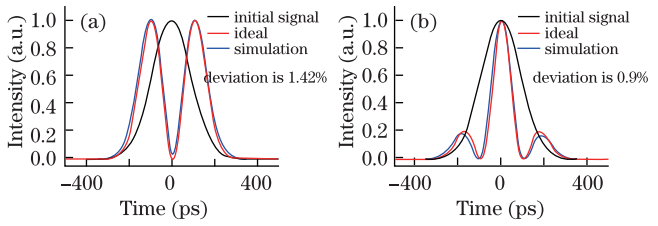

Fig. 2. (Color online) Comparison between the ideal differential signal and the output signal from the designed differentiators: (a) the first-order and (b) the second-order differentiators.

becomes narrower. Figure 1(c) shows the refractive index modulation envelope of the Moiré fiber grating designed for the second-order differentiator. Two π-phase shifted points are symmetrically located along the fiber axis. The periods of the phase mask were chosen as 535.466 and 535.523 nm. Therefore, the period of slowly varying profile was approximately equal to the length of fiber grating. Figure 1(d) shows the reflection amplitude and phase of the Moiré fiber grating. From Fig. 1(d), we can see that no π-phase jump is present in the center frequency.

In order to verify the performances of the designed first- and second-order differentiators, we simulated an initial optical signal passing through the designed differentiators. The waveform of the initial pulse is chosen as a transform-limited Gaussian pulse; therefore, the expression of the initial pulse can be written as

$$\begin{cases} E(t) = E_0 \exp\left[-\frac{1}{2}\left(\frac{t}{\tau}\right)^2\right] \\ E(\omega) = \int_{-\infty}^{+\infty} E(t)\exp[-\mathrm{i}\omega t]\mathrm{d}t \end{cases}, \tag{4}$$

where E_0 is the amplitude of the pulse and τ is the half pulse width at the e^{-1} intensity point. Conventionally, the bandwidth of the initial pulse should be narrower than the bandwidth of the reflection dip, and the center frequency must equal the frequency of zero reflection point exactly. The half pulse width τ was chosen as 100 ps. Accordingly, the spectral bandwidth of the initial pulse was narrower than the bandwidth of the reflection dip.

Figure 2 shows the simulation results of the temporal responses of the first-order and second-order differentiators. The differential temporal waveform can be calculated from the output frequency waveform of the Moiré fiber grating by inverse Fourier transform. The output frequency waveform was calculated by multiplying the amplitude of the initial pulse and the spectral response of the Moiré fiber grating. A good waveform match was easily found between the ideal differential signal (drawn with red solid line in Fig. 2) and the output temporal waveform achieved from the Moiré fiber grating (drawn with blue solid line in Fig. 2) for both of the first- and second-order temporal differentiators. The temporal profile of the input signal is drawn as a black line in Fig. 2. The deviation of the differentiator is calculated by

$$\mathrm{Dev} = \frac{\int_{-\infty}^{\infty} |E_{\mathrm{sim}}(t) - E_{\mathrm{ideal}}(t)|^2 \,\mathrm{dt}}{\int_{-\infty}^{\infty} |E_{\mathrm{ideal}}(t)|^2 \,\mathrm{dt}}. \tag{5}$$

The deviations were approximately 1.42% and 0.9% for the first- and the second-order differentiators, respectively. In actuality, the deviation of the differentiator is related to the bandwidth of the initial pulse. The deviation will become larger when the bandwidth of the initial pulse becomes wider as result of the deviation between the required linear amplitude response and the amplitude response of the Moiré fiber grating becoming larger. However, we believe that, when the bandwidth is narrower than the bandwidth of the reflection dip, the resulting deviation will be small. The simulation results verify the feasibility, flexibility, and accuracy of our proposed method.

In order to verify the feasibility of this method, we fabricated a Moiré fiber grating using two optical gratings with slightly different periods in a single optical fiber using the phase mask method. The UV beam was focused by a cylindrical lens to radiate a uniform phase mask on top of a photosensitive optical fiber. We first fabricated a uniform fiber grating in a photosensitive optical fiber approximately 30-mm long. The second fiber grating was superimposed in the same optical fiber by pulling the fiber to a longer length using a fine mechanism. The period of the second fiber grating was controlled by changing the pulling force of the mechanism. A real-time monitoring system was used to measure the spectrum response of the Moiré fiber grating. A satisfactory Moiré fiber grating could be fabrication by real-time control of the fine mechanism. Only one π-phase shift point was introduced in our fabrication. The spectrum response of the Moiré fiber grating was measured (see Fig. 3). As shown in Fig. 3, the resonance dip of the Moiré fiber grating is located at 1 548.04 nm and the operational bandwidth of the reflection dip is approximately 0.2 nm.

Based on the prepared Moiré fiber grating, we built a platform to measure the temporal response of Moiré fiber grating. An optical pulse was generated from a mode-locking fiber laser with saturable absorbency. The center wavelength of the fiber laser can control the location of the resonance dip of the Moiré fiber grating approximately by tuning the two polarization controllers in the fiber laser. Actually, the temporal waveform of the laser pulse cannot be easily directly measured by an oscilloscope because of the short time window of the pulse. An autocorrelator[20] was used to measure the temporal waveform (see Fig. 4). Figure 4 also shows the Gaussian fitting curve of the input pulse. The input pulse, which can be considered as an ideal Gaussian pulse, has

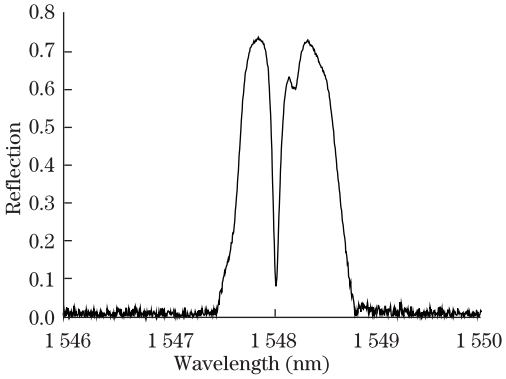

Fig. 3. Spectral response of the Moiré fiber grating.

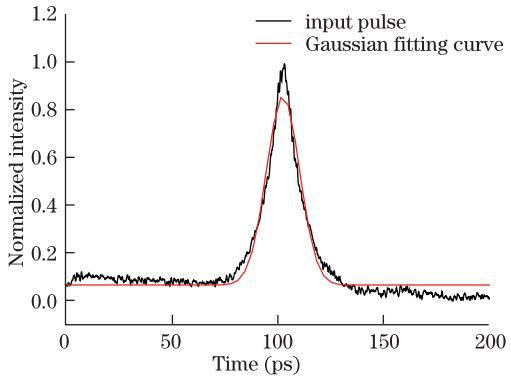

Fig. 4. Autocorrelation trace of the input pulse.

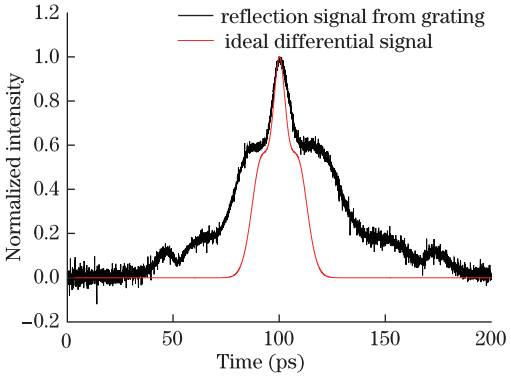

Fig. 5. (Color online) Autocorrelation trace of the ideal differential signal and reflection signal from Moiré fiber grating.

a pulse width of approximately 15.6 ps. The optical pulse passes through the Moiré fiber grating; thus, the reflection pulse can be obtained by an optical circulator. Using this method, the autocorrelation trace of the reflection signal achieved from the Moiré fiber grating is measured, and is drawn as a black solid line in Fig. 5. The autocorrelation trace of the ideal differential signal is also displayed as a red solid line in Fig. 5 for comparison. Figure 5 shows a basic waveform match between the ideal differential signal and the temporal signal reflected from the Moiré fiber grating. The deviation here is much larger than in the simulation result due to the non-zero reflection dip of the prepared Moiré fiber grating introduced in the resonance dip and the limited operational bandwidth of the Moiré fiber Bragg grating.

In conclusion, we design and demonstrat a single Moiré fiber grating to realize an all-fiber temporal differentiator. The first- and second-order temporal differentiators are designed as examples. The first-order temporal differentiator is realized by a Moiré fiber grating with only one π-phase shifted point. The second-order temporal differentiator is achieved by a Moiré fiber grating incorporating two symmetrical π-phase shifted points. A good waveform match is achieved between the ideal differential signal and the output temporal waveform achieved from the Moiré fiber grating for both of the first- and second-order temporal differentiators.

This work was supported by the National Natural Science Foundation of China (No. 60871067), the National Natural Science Association Foundation of China (No. 11076028), and the Projects of Science and Technology Commission of Shanghai Municipality (No. 08DZ2230400).

References

1. F. X. Li, Y. Park, and J. Azana, Opt. Lett. **32,** 3364 (2007).
2. F.X. Li, Y. Park, and J. Azana, in *Proceedings of Optical Fiber Communication/National Fiber Optic Engineers Conference* **1-8,** 2606 (2008).
3. Y. Park, M. Kulishov, R. Slavik, and J. Azana, Opt. Express **14,** 12670 (2006).
4. R. Slavik, Y. Park, and J. Azana, Opt. Express **15,** 6717 (2007).
5. N. Q. Ngo , S. F. Yu, S. C. Tjin, and C. H. Kam, Opt. Commun. **230,** 115 (2004).
6. R. Slavik, Y. Park, M. Kulishov, R. Morandotti, and J. Azana, Opt. Express **14,** 10699 (2006).
7. M. Li, D. Janner, J. P. Yao, and V. Pruneri, Opt. Express **17,** 19798 (2009).
8. J. Xu, X. L. Zhang, J. J. Dong, D. M. Liu, and D. X. Huang, Opt. Lett. **32,** 3029 (2007).
9. J. Xu, X. L. Zhang, J. J. Dong, D. M. Liu, and D. X. Huang, Opt. Lett. **32,** 1872 (2007).
10. F. F. Liu, T. Wang, L. Qiang, T. Ye, Z. Zhang, W. Qiu, and Y. Su, Opt. Express **16,** 15880 (2008).
11. M. Kulishov and J. Azana, Opt. Lett. **30,** 2700 (2005).
12. M. Kulishov, D. Krcmarik, and R. Slavik, Opt. Lett. **32,** 2978 (2007).
13. R. Slavik, Y. Park, D. Krcmarik, and J. Azana, Opt. Commun. **282,** 2339 (2009).
14. T. Cai, Y. Liu, X. Zhang, and T. Wang, Chin. Opt. Lett. **9,** 041403 (2011)
15. C. Cuadrado-Laborde, Opt. Quantum Electron. **40,** 983 (2008).
16. C. Cuadrado-Laborde and M. V. Andres, Opt. Lett. **34,** 833 (2009).
17. M. Li , L. Y. Shao, J. Albert, and J. P. Yao, IEEE Photon. Technol. Lett. **23,** 251 (2011).
18. L. M. Rivas, K. Singh, A. Carballar, and J. Azana, IEEE Photon. Technol. Lett. **19,** 1209 (2007).
19. L. Zhao, L. Li, A. P. Luo, J. Z. Xia, R. H. Qu, and Z. J. Fang, Optik **113,** 464 (2002).
20. Q. Xu, Q. Liu, Q. Ye, Z. Pan, H. Cai, Z. Fang, and R. Qu, Chinese J. Lasers (in Chinese) **37,** 6 (2010).